[1.]Mihai ȚĂLU, [2.]Ștefan ȚĂLU

OPTIMAL ENGINEERING DESIGN OF A PRESSURIZED PARALEPIPEDIC FUEL TANK

[1.] University of Craiova, Faculty of Mechanics, Applied Mechanics and Civil Engineering, Craiova, ROMANIA
[2.] Technical University of Cluj-Napoca, Development and Innovation Management (DMCDI), Cluj-Napoca, ROMANIA

Abstract: The goal of this research was to evaluate the optimal geometry of a pressurized paralepipedic fuel tank with the finite element analysis (FEA). Geometrical modeling was done in the AutoCAD Autodesk 2017 software and its stress-strain state calculation was done using the SolidWorks 2017 software for both thermal and mechanical events. In numerical analysis, polynomial interpolation was applied to determine variation laws of the von Mises stress and linear deformation distribution. The relationship between properties and loading conditions can be utilized to optimize the fabrication process to obtain high quality products. The computational analysis results revealed that the pressurized paralepipedic fuel tank satisfies the design regulations and can be applicable for use in automotive industry.
Keywords: automotive industry, industrial engineering design, optimization, pressurized paralepipedic fuel tank

1. INTRODUCTION

During the past few decades, the computer aided engineering (CAE) tools [1-3] are very widely used in the automotive industry to reduce product development cost and time while improving the safety, comfort, and durability [4-7].

CAE tools include simulation, validation and optimization of products, processes, and manufacturing tools to help support design teams in decision making that would be difficult to obtain any other way [8-14].

On the other hand, finite element analysis (FEA) and computational fluid dynamics (CFD) allow efficient simulation of 3-D geometrical vehicle models, to reduce physical build-and-test experiments, shorten time to market and reduce financial risks [15, 16].

The storage fuel tanks are used in the automotive industry for safely storing fuel: compressed natural gas (CNG) or liquefied petroleum gas (LPG) [15-17]. The most common materials used in the manufacture of storage fuel tanks are aluminum alloys and various types of steel [15].

The design, construction, installation, testing and monitoring requirements of the storage fuel tanks, fabricated in a combination of various shapes are available in various codes and international standards that includes a comprehensive set of requirements in the following areas: construction requirements; performance tests; markings and production line test [18].

The multi-objective optimization technique of the fuel tanks to determine critical design parameters and to perform design optimization involves different assumptions and simplifications, mathematical formulations, supershapes design variables [19, 20], specific structure parameters [8-14], geometrical conditions [15], design constraints [2-5], computer tools [21-26], numerical computational methods [27-29], CAD visualization techniques [30-36], measurement methods [37], test data and experimental data.

Various studies have been devoted to the Von Mises stress and linear deformation distribution of the fuel tank walls and the heat transfer across the fuel tank walls in non-linear analysis, both experimentally and numerically [8-14, 15-17].

In this research, a finite element analysis has been chosen to optimize the specific geometry of structure parameters of pressurized paralepipedic fuel tanks.

2. DESIGN METHODOLOGY

In our study, an optimal design of pressurized paralepipedic fuel tanks (considering shape and thickness variation) in order to reduce stress non-uniformity concentration is performed.

⧉ The geometrical model selected for numerical analysis

The geometrical model selected for numerical analysis is shown in Figure 1.

The modeling was done in the AutoCAD Autodesk 2017 software [38] and the optimization analysis to ensure quality, performance, and safety was performed with SolidWorks 2017 software [39] with the: Static, Thermal and Design Study modules.

Figure 1. The geometrical model of pressurized paralepipedic fuel tank

The design data used in this analysis for pressurized paralepipedic fuel tank are (Figure 1):

- the head cap is flat with the following dimensions: L = 200 mm;
- the lateral cover has the following dimensions: width B = 200 mm and length L = 800 mm;
- the maximum static hydraulic pressure: p_{max} = 20 bar;
- the working temperature between the limits: T = -30 ^{0}C to T = 60 ^{0}C;
- the execution material for tank is AISI4340 laminated steel;
- the exploitation time of tank is: n_a = 15 years;
- the corrosion velocity of material: v_c = 0.05 mm/year.

The CAD design of the lateral cover

The parameterized model used in calculus is a section of ¼ from the initial cover (Figure 2) and the corresponding surfaces to which the constraints and restrictions are applied are shown in Figure 3.

The design data used in this analysis for the tank lateral cover are:

- the maximum pressure p_{max} = 20 bar on the inner surface S_5;
- the execution material of lateral cover is AISI4340 laminated steel;
- the working temperature between the limits: T = -30 ^{0}C to T = 60 ^{0}C on the surface S_6;
- the opposing and equal traction forces of value of F = 20000 N on the surfaces: S_1 and S_2, generated by the action of pressure on the inner surfaces of the head covers;
- the surface symmetry on S_3 and S_4;
- the fixation of the S_7 surface on the tank supports.

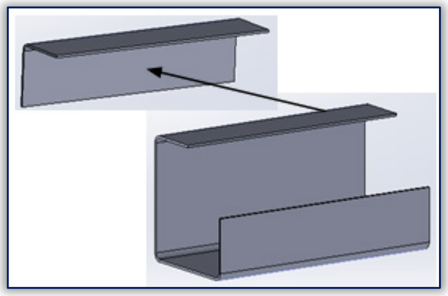

Figure 2. The quarter section of parametric model

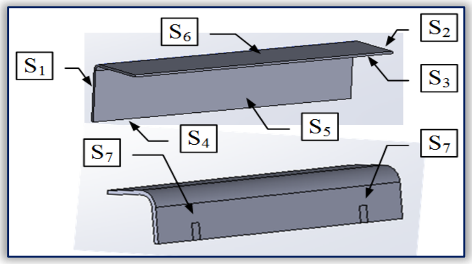

Figure 3. The quarter section of parametric model where is made the marking of the exterior surfaces

The lateral cover is optimized to obtain a minimum mass and the effort must be: $\sigma_{rez} \leq \sigma_a$ =710 N/mm^2.
The sizes to be optimized are: the thickness of lateral cover s = 5...8 mm and the connection radius between the sides of lateral cover R = 30 mm. The obtained values are: s = 6.68 mm at T = -30 ^{0}C for the maximum effort $\sigma_{rez.\,max}$ = 709.3 N/mm^2 and the linear deformation u_{max} = 1.917 mm.

The distribution of the stress and linear deformation of the optimal lateral cover is shown in Figure 4.

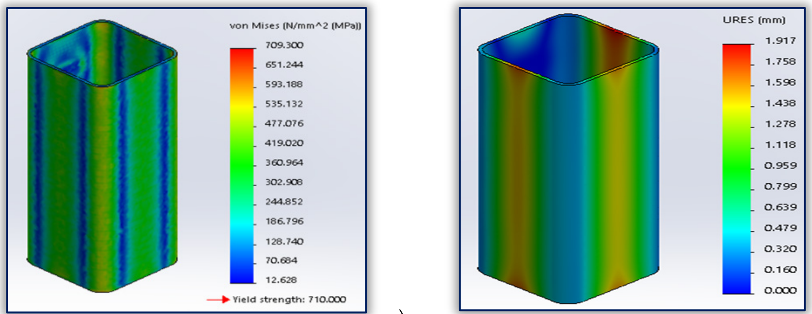

a) b)

Figure 4. The graphs for lateral cover: a) The Von Mises stress; b) The resultant linear deformation

The optimal thickness is corrected considering the influence of the corrosion phenomenon and the negative tolerance of the metal sheet, using the following formula [10]:

$$s_{real} = s_{opt} + \Delta s_c + \Delta s_T + \Delta s_{am} = s_{opt} + v_c \cdot n_a + abs(A_i) + 0.1 \cdot s \quad (1)$$

where:

- Δs_c, the additional thickness used to compensate the loss of thickness due to the corrosion process;
- Δs_T, the additional thickness used to compensate the loss due to the negative tolerance of the execution of laminate metal sheet;
- v_c, the corrosion velocity of the metal sheet, $v_c = 0.05$ mm/year;
- n_a, the number of years of exploitation, $n_a = 15$ years;
- A_i, the negative tolerance of the laminate sheet, $A_i = - 0.6$ mm;
- $\Delta s_{am} = 0.1 \cdot s$, the additional thickness used to compensate the thinning of wall into the embossing process, $\Delta s_{am} = 0.8$ mm.

By substituting the numerical values, the minimum thickness of the laminate sheet has the following value:

$$s_{real\ min} = 6.68 + 0.05 \cdot 15 + abs(-0.6) + 0.1 \cdot 8 = 8.83 \text{ mm} \quad (2)$$

For the execution, we choose a laminate sheet of AISI 4340 steel that has a thickness of $s = 9^{+0.25}_{-0.6}$ mm.

The CAD design of the head cover

The sketch of the head cover (Figure 5) has the following notations: D - the size of the square; s – the cover thickness; r – the connection radius; h – the height of straight flange and H – the total height of the head cover.

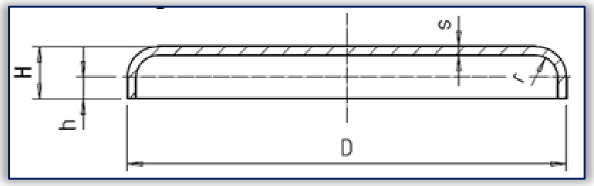

Figure 5. The sketch of the head cover

The three-quarter section of head cover parameterized model is shown in Figure 6 and the corresponding surfaces to which the constraints and restrictions are applied are shown in Figure 7.

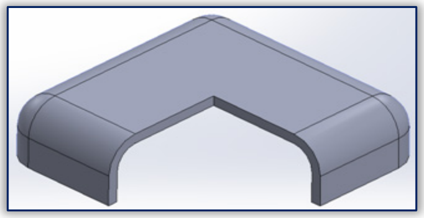

Figure 6. The three-quarter section of head cover

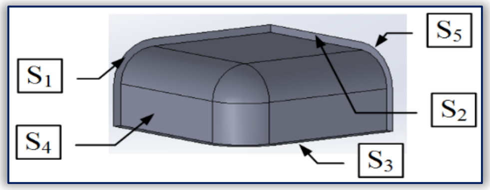

Figure 7. The quarter section of head cover where is made the marking of the exterior surfaces

The design data used in this analysis for the tank head cover are:

- the maximum pressure $p_{max} = 20$ bar on the inner surface S_4;
- the working temperature between the limits: T = -30 ^{0}C to T = 60 ^{0}C on the surface S_5;
- the surface symmetry on S_1 and S_2;
- the execution material of head cover is AISI4340 laminated steel.

The head cover is optimized to obtain a minimum mass and the effort must be: $\sigma_{rez} \le \sigma_a = 710$ N/mm^2.

The sizes to be optimized are: the thickness of head cover s = 2...4 mm and the height of straight flange h = 3.5·s. The obtained values are: s = 4.35 mm, h = 16 mm at T = -30 ^{0}C for the maximum effort $\sigma_{rez.\ max} = 704.77$ N/mm^2 and the linear deformation $u_{max} = 2.008$ mm.

The distribution of the stress and linear deformation of the optimal head cover is shown in Figure 8.

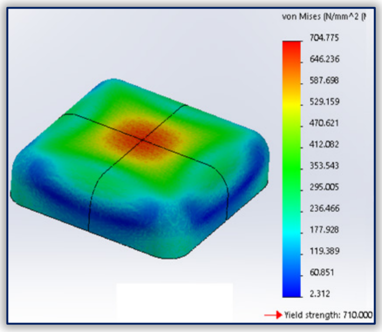

a)

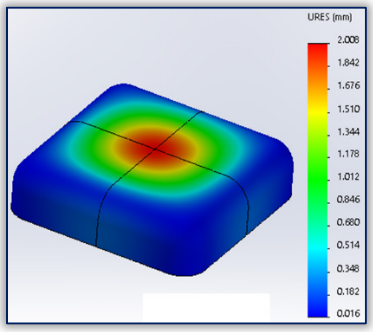

b)

Figure 8. The graphs for head cover: a) The Von Mises stress; b) The resultant linear deformation

The minimum real thickness of the head cover is:

$$s_{real\ min} = 4.35 + 0.05 \cdot 15 + abs(-0.6) + 0.1 \cdot 7 = 6.4 \text{ mm} \quad (3)$$

A laminate sheet of AISI 4340 steel with a thickness of $s = 6.5^{+0.25}_{-0.6}$ mm was chosen.

Three-dimensional stress and strain analysis

The graphs of stress and linear deformation distribution of tank at T = -30 ^{0}C are shown for: a) n_a = 0 years, $\sigma_{rez.\ max}$ = 435.87 N/mm^2, u_{max} = 0.450 mm (in figs. 9a and 9b); b) n_a = 15 years, $\sigma_{rez.\ max}$ = 683.54 N/mm^2, u_{max} = 1.803 mm (in figs. 9c and 9d).

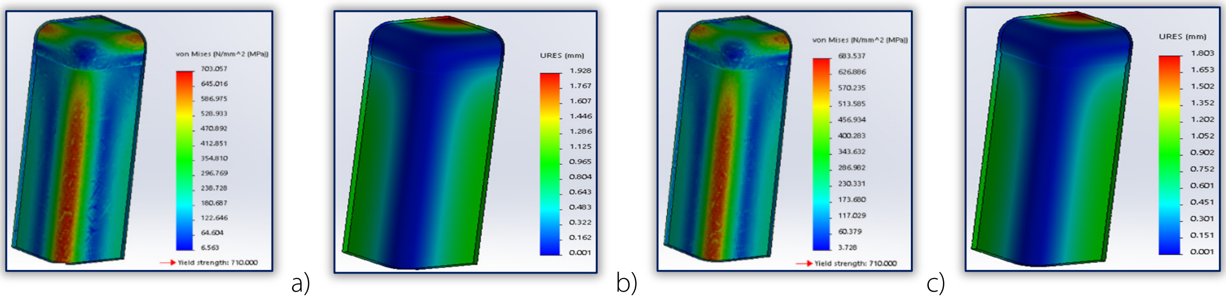

a) b) c) d)

Figure 9. The graphs of: I) a) Von Mises stress distribution and b) linear deformation distribution, both computed for n_a = 0 years, T = -30 ^{0}C; c) Von Mises stress distribution and d) linear deformation distribution, both computed for n_a = 15 years, T = -30 ^{0}C.

It can be revealed that at n_a = 15 years: I) in lateral cover, the thickness is s = 4.45 mm, compared to optimized thickness s = 4.35 mm; II) in head cover, the thickness is s = 6.85 mm, compared to optimized thickness s = 6.68 mm.

The graphs of Von Mises stress and linear deformation for lateral cover, computed along of a specified line, for n_a = 15 years, T = -30 ^{0}C, is shown in Figure 10b and 10c.

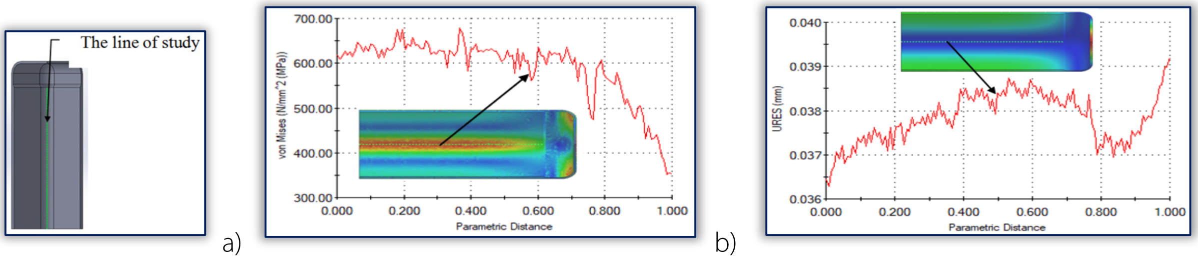

a) b) c)

Figure 10. a) The geometrical model of lateral cover; The graphs of Von Mises stress distribution (b) and linear deformation (c), computed along of a specified line, for n_a = 15 years, T = -30 ^{0}C.

The graphs of Von Mises stress and linear deformation for head cover, computed along of a specified line parallel with the boundary edges, for n_a = 15 years, T = -30 ^{0}C, is shown in Figure 11b and 11c.

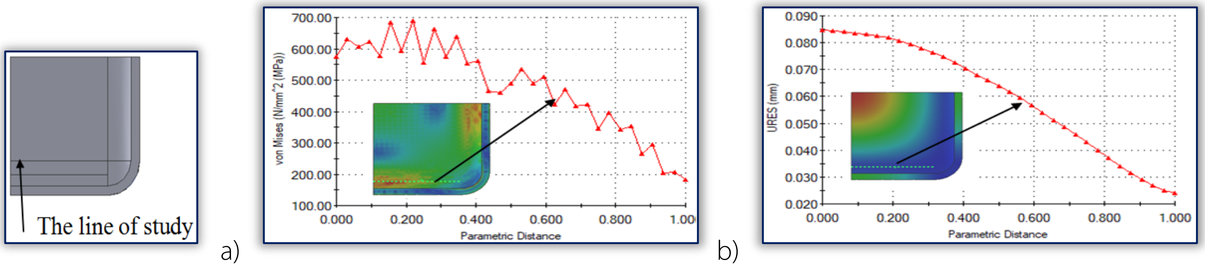

a) b) c)

Figure 11. a) The geometrical model of head cover; The graphs of Von Mises stress distribution (b) and linear deformation (c), computed along of a specified line parallel with the boundary edges, for n_a = 15 years, T = -30 ^{0}C.

The graphs of Von Mises stress and linear deformation for head cover, computed along of a specified line located on bisector angle of sides, for n_a = 15 years, T = -30 ^{0}C, is shown in Figure 12b and 12c.

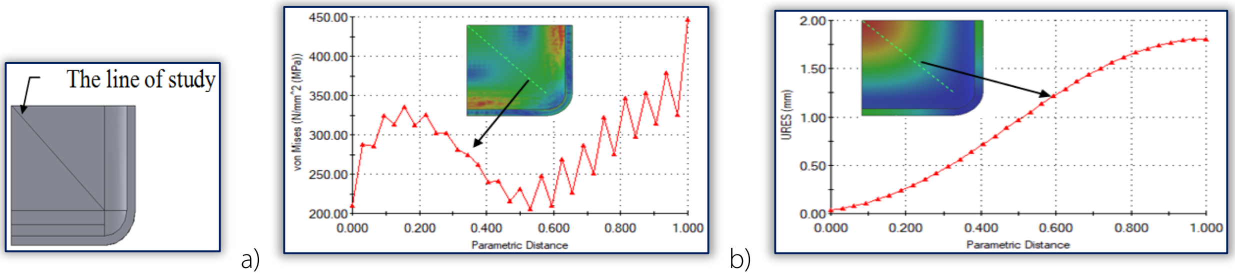

a) b) c)

Figure 12. a) The geometrical model of head cover; The graphs of Von Mises stress distribution (b) and linear deformation (c), computed along of a specified line located on bisector angle of sides, for n_a = 15 years, T = -30 ^{0}C.

The numerical values of Von Mises stress and linear deformation distribution of pressurized paralepipedic fuel tank during the period of exploitation are given in Table 1.

Table 1. The Von Mises stress and linear deformation during the period of exploitation

n_a		T [^{0}C]									
		-30	-20	-10	0	10	20	30	40	50	60
1	σ [MPa]	593.41	571.15	549.21	527.65	506.50	485.82	468.84	460.09	461.04	463.81
	u [mm]	1.148	1.153	1.159	1.164	1.170	1.175	1.181	1.186	1.192	1.197
2	σ [MPa]	595.08	574.15	553.50	533.18	513.21	493.65	482.15	483.79	485.47	487.19
	u [mm]	1.203	1.209	1.214	1.219	1.224	1.229	1.234	1.239	1.245	1.250
4	σ [MPa]	607.29	585.62	564.32	543.42	522.97	503.7	495.03	486.57	486.95	488.73
	u [mm]	1.259	1.264	1.269	1.275	1.28	1.285	1.29	1.296	1.301	1.306
6	σ [MPa]	647.86	620.50	593.45	566.74	540.43	517.59	512.57	512.12	512.42	515.56
	u [mm]	1.34	1.345	1.351	1.356	1.361	1.366	1.371	1.376	1.381	1.378
8	σ [MPa]	651.81	626.91	602.29	577.99	554.06	531.36	527.50	524.93	525.66	526.58
	u [mm]	1.43	1.434	1.439	1.444	1.449	1.454	1.459	1.464	1.469	1.474
10	σ [MPa]	651.33	627.82	604.56	583.20	563.77	551.30	548.13	545.36	543.08	540.88
	u [mm]	1.525	1.530	1.535	1.540	1.545	1.550	1.555	1.559	1.564	1.569
12	σ [MPa]	707.53	684.82	662.37	640.24	618.43	596.99	575.97	569.85	565.39	568.51
	u [mm]	1.634	1.638	1.642	1.646	1.650	1.654	1.658	1.662	1.666	1.670
15	σ [MPa]	683.53	660.57	637.89	615.70	611.31	607.80	604.35	605.85	607.36	608.90
	u [mm]	1.803	1.808	1.812	1.817	1.822	1.827	1.832	1.836	1.841	1.846

The graphs of Von Mises stress and linear deformation are shown in Figure 13 and 14 with the corresponding laws of variation computed by polynomial interpolation.

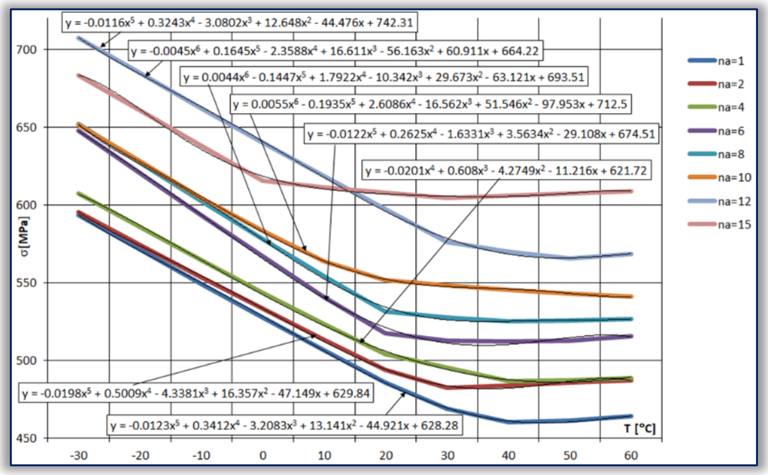

Figure 13. The graphs of Von Mises stress variation with the corresponding laws of variation computed by polynomial interpolation

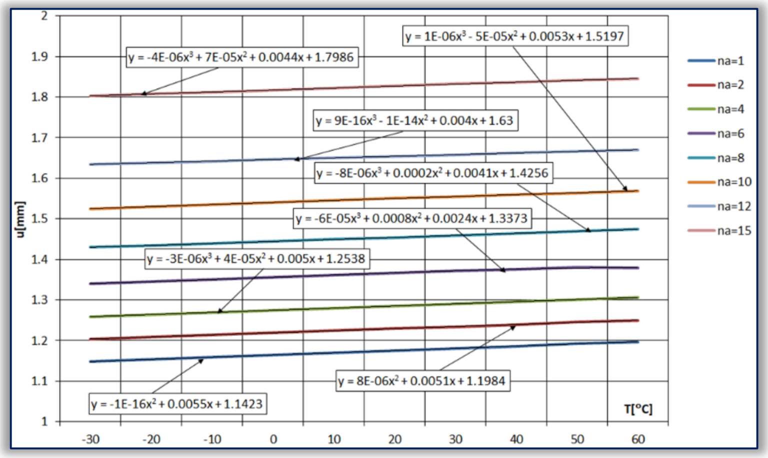

Figure 14. The graphs of linear deformation with the corresponding laws of variation computed by polynomial interpolation

The graphs of Von Mises stress and linear deformation (for n_a = 15 years) are shown in Figure 15a and 15b with the corresponding laws of variation computed by polynomial interpolation.

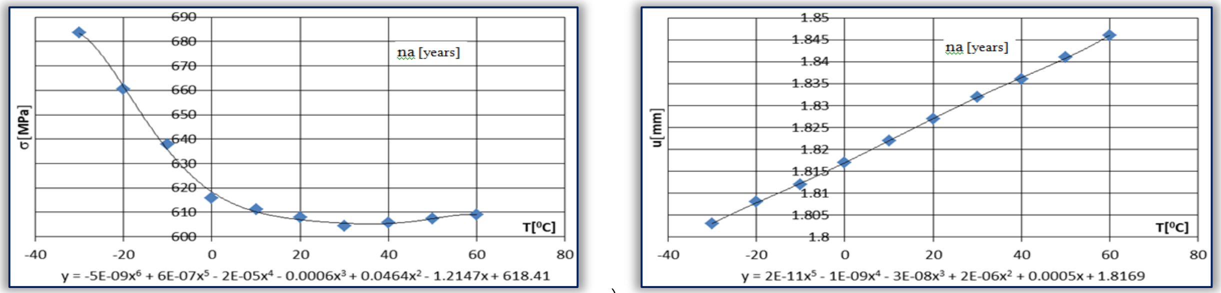

a) b)

Figure 15. The graphs of Von Mises stress (a) and linear deformation (b) at n_a = 15 years

The graphical representations of Von Mises stress σ = (n_a, T) and the linear deformation, u (n_a, T) as specified in Table 1, are shown in Figure 16a and 16b.

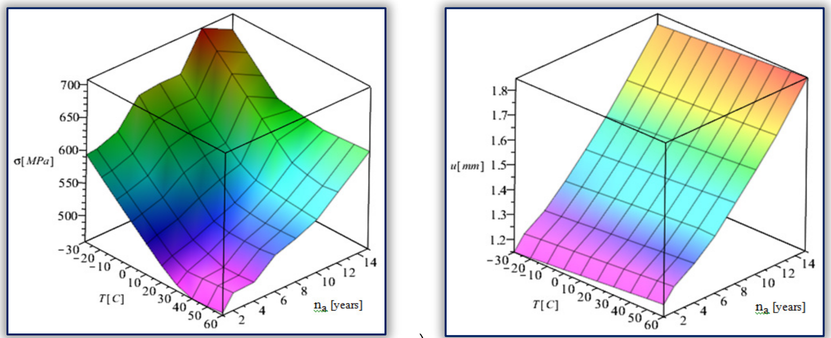

a) b)

Figure 16. The graphs of: a) Von Mises stress σ = (n_a, T) and b) linear deformation u (n_a, T)

The graphs of Von Mises stress and linear deformation distribution of tank (for n_a = 15 years) are shown for: a) the maximum temperature T_{max} = 143.7 ^{0}C (in figs. 17a and 17b); b) the explosion temperature T_r = 316.5 ^{0}C (in figs. 17c and 17d).

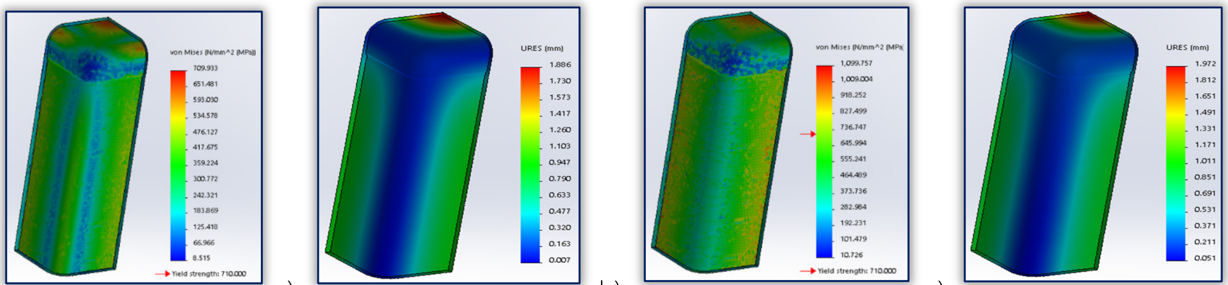

a) b) c) d)

Figure 17. The graphs of: I) a) Von Mises stress distribution and b) linear deformation distribution, both computed for n_a = 15 years, T_{max} = 143.7 ^{0}C; c) Von Mises stress distribution and d) linear deformation distribution, both computed for n_a = 15 years, T_r = 316.5 ^{0}C.

3. DISCUSSIONS

It can be seen that the maximum stress appears in different locations of tank (as shown in Figure 9 to 12). It is also found that the effective stresses and deformations are lower than the imposed values obtained in CAD optimal design, (as shown in Table 1).

It can be revealed that for n_a = ct., the Von Mises stress decreases with the increasing of temperature (from T = -30 ^{0}C to T = 40 ^{0}C), then increases from T = 40 ^{0}C to T = 60 ^{0}C (as shown in Figure 13). In the same time, without exception all graphs show a minimum value.

On the other hand, all the linear deformations increases with the increasing of temperature (from T = -30 ^{0}C to T = 60 ^{0}C) (as shown in Figure 14).

In the last year of exploitation (n_a = 15 years), the maximum value of the Von Mises stress (σ = 683.53 MPa) occurs at T = - 30 ^{0}C, while the minimum value of the Von Mises stress (σ = 604.35 MPa) occurs at T = 30 ^{0}C (as shown in Figure 15a). In the same time (n_a = 15 years), the maximum linear deformation (u_{max} = 1.846 mm) occurs at T = 60 ^{0}C, while the minimum linear deformation (u_{max} = 1.803 mm) occurs at T = -30 ^{0}C (as shown in Figure 15b).

4. CONCLUSIONS

In this study, an elaboration of the design and optimization procedure associated with the pressurized paralepipedic fuel tanks used in automotive industry based on the FEA approaches were performed.

Computer aided investigations, based on the mechanical characteristic of the material components, were employed to predict the mechanical behavior of paralepipedic fuel tanks, corresponding to various design scenarios under a prescribed set of conditions, in order to improve the fuel storage capacity.

The combination of design criteria into quantifiable objective functions, from the model equations with the minimum number of appropriate design variables would also be considered as design objectives in the future areas of pressurized paralepipedic fuel tanks.

Financial disclosure:

Neither author has a financial or proprietary interest in any material or method mentioned.

Competing interests:

The authors declare that they have no significant competing financial, professional or personal interests that might have influenced the performance or presentation of the work described in this manuscript.

References

[1] M. Hirz, W. Dietrich, A. Gfrerrer, J. Lang, Integrated Computer-Aided Design in Automotive Development, Springer-Verlag Berlin Heidelberg, 2013. DOI: 10.1007/978-3-642-11940-8

[2] M.C. Ghiţă, A.C. Micu, M. Ţălu, Ş. Ţălu, E. Adam, Computer-Aided Design of a classical cylinder gas tank for the automotive industry, Annals of Faculty of Engineering Hunedoara - International Journal of Engineering, Hunedoara, Tome XI, Fascicule 4, pp. 59-64, 2013

[3] M.C. Ghiţă, A.C. Micu, M. Ţălu, Ş. Ţălu, 3D modelling of a gas tank with reversed end up covers for automotive industry, Annals of Faculty of Engineering Hunedoara - International Journal of Engineering, Hunedoara, Tome XI, Fascicule 3, 2013, pp. 195-200, 2013

[4] M.C. Ghiţă, A.C. Micu, M. Ţălu, Ş. Ţălu, Shape optimization of vehicle's methane gas tank, Annals of Faculty of Engineering Hunedoara - International Journal of Engineering, Hunedoara, Tome X, Fascicule 3, pp. 259-266, 2012

[5] M.C. Ghiţă, A.C. Micu, M. Ţălu, Ş. Ţălu, 3D modelling of a shrink fitted concave ended cylindrical tank for automotive industry. Acta Technica Corviniensis – Bulletin of Engineering, Hunedoara, Romania, Tome VI, Fascicule 4, pp. 87-92, 2013

[6] M.C. Ghiţă, C.Ş. Ghiţă, Ş. Ţălu, S. Rotaru, Optimal design of cylindrical rings used for the shrinkage of vehicle tanks for compressed natural gas, Annals of Faculty of Engineering Hunedoara - International Journal of Engineering, Hunedoara, Tome XII, Fascicule 3, pp. 243-250, 2014

[7] M.C. Ghiţă, A.C. Micu, M. Ţălu, Ş. Ţălu, Shape optimization of a thoroidal methane gas tank for automotive industry, Annals of Faculty of Engineering Hunedoara - International Journal of Engineering, Hunedoara, Tome X, Fascicule 3, pp. 295-297, 2012

[8] M. Bică, M. Ţălu, Ş. Ţălu, Optimal shapes of the cylindrical pressurized fuel tanks, Magazine of Hydraulics, Pneumatics, Tribology, Ecology, Sensorics, Mechatronics (HIDRAULICA), no. 4, pp. 6-17, 2017

[9] Ş. Ţălu, M. Ţălu, The influence of deviation from circularity on the stress of a pressurized fuel cylindrical tank, Magazine of Hydraulics, Pneumatics, Tribology, Ecology, Sensorics, Mechatronics (HIDRAULICA), no. 4, pp. 34-45, 2017.

[10] D. Vintilă, M. Ţălu, Ş. Ţălu, The CAD analyses of a torospheric head cover of a pressurized cylindrical fuel tank after the crash test, Magazine of Hydraulics, Pneumatics, Tribology, Ecology, Sensorics, Mechatronics (HIDRAULICA), no. 4, pp. 57-66, 2017

[11] M. Ţălu, The influence of the corrosion and temperature on the Von Mises stress in the lateral cover of a pressurized fuel tank, Magazine of Hydraulics, Pneumatics, Tribology, Ecology, Sensorics, Mechatronics (HIDRAULICA), no. 4, pp. 89-97, 2017

[12] M. Ţălu, Ş. Ţălu, Analysis of temperature resistance of pressurized cylindrical fuel tanks, Magazine of Hydraulics, Pneumatics, Tribology, Ecology, Sensorics, Mechatronics (HIDRAULICA), no. 1, pp. 6-15, 2018.

[13] M. Ţălu, Ş. Ţălu, Design and optimization of pressurized toroidal LPG fuel tanks with variable section, Magazine of Hydraulics, Pneumatics, Tribology, Ecology, Sensorics, Mechatronics (HIDRAULICA), no. 1, 2018.

[14] Ş. Ţălu, M. Ţălu, Algorithm for optimal design of pressurized toroidal LPG fuel tanks with constant section described by imposed algebraic plane curves, Magazine of Hydraulics, Pneumatics, Tribology, Ecology, Sensorics, Mechatronics (HIDRAULICA), no. 1, 2018

[15] P.M. Patel, R. Jaypalsinh, Design & optimization of LNG-CNG cylinder for optimum weight, IJSRD - International Journal for Scientific Research & Development, vol. 1, issue 2, pp. 282-286, 2013

[16] G. Remya, Gopi, B.R. Beena, Finite Element Analysis of GFRP LPG cylinder, IJEDR, vol. 3, issue 4, pp. 642-649, 2015

[17] T. Izaki, Y. Sueki, T. Mizuguchi, M. Kurosaki, New steel solution for automotive fuel tanks, Rev. Met. Paris, Vol. 102, no. 9, pp. 613-619, 2005
[18] *** Certification tests of LPG and CNG (available at site http://vzlutest.cz/en/certification-tests-of-lpg-and-cng-c3.html)
[19] Ş. Ţălu, M. Ţălu, CAD generating of 3D supershapes in different coordinate systems, Annals of Faculty of Engineering Hunedoara - International Journal of Engineering, Hunedoara, Tome VIII, Fascicule 3, pp. 215-219, 2010
[20] Ş. Ţălu, M. Ţălu, A CAD study on generating of 2D supershapes in different coordinate systems, Annals of Faculty of Engineering Hunedoara - International Journal of Engineering, Hunedoara, Tome VIII, Fascicule 3, pp. 201-203, 2010
[21] Ş. Ţălu, Limbajul de programare AutoLISP. Teorie şi aplicaţii, (AutoLISP programming language. Theory and applications), Cluj-Napoca, Risoprint Publishing house, 2001
[22] Ş. Ţălu, Grafică tehnică asistată de calculator (Computer assisted technical graphics), Cluj-Napoca, Victor Melenti Publishing house, 2001
[23] Ş. Ţălu, Reprezentări grafice asistate de calculator (Computer assisted graphical representations), Cluj-Napoca, Osama Publishing house, 2001
[24] Ş. Ţălu, AutoCAD 2005, Cluj-Napoca, Risoprint Publishing house, 2005
[25] Ş. Ţălu, M. Ţălu, AutoCAD 2006. Proiectare tridimensională (AutoCAD 2006. Three-dimensional designing), Cluj-Napoca, MEGA Publishing house, 2007
[26] Ş. Ţălu, AutoCAD 2017, Cluj-Napoca, Napoca Star Publishing house, 2017
[27] M. Ţălu, Calculul pierderilor de presiune distribuite în conducte hidraulice (Calculation of distributed pressure loss in hydraulic pipelines), Craiova, Universitaria Publishing house, 2016
[28] M. Ţălu, Pierderi de presiune hidraulică în conducte tehnice cu secţiune inelară. Calcul numeric şi analiză C.F.D. (Hydraulic pressure loss in technical piping with annular section. Numerical calculation and C.F.D.), Craiova, Universitaria Publishing house, 2016
[29] M. Ţălu, Mecanica fluidelor. Curgeri laminare monodimensionale (Fluid mechanics. The monodimensional laminar flow), Craiova, Universitaria Publishing house, 2016
[30] Ş. Ţălu, Geometrie descriptivă (Descriptive geometry), Cluj-Napoca, Risoprint Publishing house, 2010
[31] A. Florescu-Gligore, M. Orban Ş. Ţălu, Cotarea în proiectarea constructivă şi tehnologică (Dimensioning in technological and constructive engineering graphics), Cluj-Napoca, Lithography of The Technical University of Cluj-Napoca, 1998
[32] A. Florescu-Gligore, Ş. Ţălu, D. Noveanu, Reprezentarea şi vizualizarea formelor geometrice în desenul industrial (Representation and visualization of geometric shapes in industrial drawing), Cluj-Napoca, U. T. Pres Publishing house, 2006
[33] Ş. Ţălu, C. Racocea, Reprezentări axonometrice cu aplicaţii în tehnică (Axonometric representations with applications in technique), Cluj-Napoca, MEGA Publishing house, 2007
[34] C. Racocea, Ş. Ţălu, Reprezentarea formelor geometrice tehnice în axonometrie (The axonometric representation of technical geometric shapes), Cluj-Napoca, Napoca Star Publishing house, 2011
[35] C. Bîrleanu, Ş. Ţălu, Organe de maşini. Proiectare şi reprezentare grafică asistată de calculator. (Machine elements. Designing and computer assisted graphical representations), Cluj-Napoca, Victor Melenti Publishing house, 2001
[36] T. Niţulescu, Ş. Ţălu, Aplicaţii ale geometriei descriptive şi graficii asistate de calculator în desenul industrial (Applications of descriptive geometry and computer aided design in engineering graphics), Cluj-Napoca, Risoprint Publishing house, 2001
[37] Ş. Ţălu, Micro and nanoscale characterization of three dimensional surfaces. Basics and applications, Napoca Star Publishing House, Cluj-Napoca, Romania, 2015
[38] *** Autodesk AutoCAD 2017 software
[39] *** SolidWorks 2017 software

ISSN 1584 - 2665 (printed version); ISSN 2601 - 2332 (online); ISSN-L 1584 - 2665
copyright © University POLITEHNICA Timisoara, Faculty of Engineering Hunedoara,
5, Revolutiei, 331128, Hunedoara, ROMANIA
http://annals.fih.upt.ro